

AD-A263 565



②

OFFICE OF NAVAL RESEARCH

Research Contract N00014-90-J-1212

R&T Code 4133008

Technical Report No. 92

"The Electrolyte Factor in O₂ Reduction Electrocatalysis"

by

E. Yeager, M. Razaq, D. Gervasio, A. Razaq and D. Tryk

Prepared for Publication

in the

Proceedings of the
Workshop on
Structural Effects in Electrocatalysis and Oxygen Electrochemistry
The Electrochemical Society
Volume No. 92-11, pp. 440-473

Department of Chemistry
Case Western Reserve University
Cleveland, Ohio 44106-7078

April 23, 1993



Reproduction in whole, or in part, is permitted for any purpose of the United States Government.

This document has been approved for public release and sale; its distribution is unlimited.

93 4 30 059

93-09286



3208

REPORT DOCUMENTATION PAGE

Form Approved
OMB No. 0704-0188

Public reporting burden for this collection of information is estimated to average 1 hour per response, including the time for reviewing instructions, searching existing data sources, gathering and maintaining the data needed, and completing and reviewing the collection of information. Send comments regarding this burden estimate or any other aspect of this collection of information, including suggestions for reducing this burden, to Washington Headquarters Services, Directorate for Information Operations and Reports, 1215 Jefferson Davis Highway, Suite 1204, Arlington, VA 22202-4302, and to the Office of Management and Budget, Paperwork Reduction Project (0704-0188), Washington, DC 20503.

1. AGENCY USE ONLY (Leave blank)		2. REPORT DATE April 23, 1993	3. REPORT TYPE AND DATES COVERED Technical (1 June 1992 - 31 May 1993)	
4. TITLE AND SUBTITLE The Electrolyte Factor in O ₂ Reduction Electrocatalysis			5. FUNDING NUMBERS C - N00014-90-J-1212 PR - 359-451	
6. AUTHOR(S) E. Yeager, M. Razaq, D. Gervasio, A. Razaq and D. Tryk				
7. PERFORMING ORGANIZATION NAME(S) AND ADDRESS(ES) Department of Chemistry Case Western Reserve University Cleveland, Ohio 44106-7078			8. PERFORMING ORGANIZATION REPORT NUMBER Technical Report No. 92	
9. SPONSORING / MONITORING AGENCY NAME(S) AND ADDRESS(ES) Office of Naval Research Chemistry Division Arlington, Virginia 22217-5000			10. SPONSORING / MONITORING AGENCY REPORT NUMBER	
11. SUPPLEMENTARY NOTES				
12a. DISTRIBUTION / AVAILABILITY STATEMENT Approved for public release and sale; its distribution is unlimited.			12b. DISTRIBUTION CODE	
13. ABSTRACT (Maximum 200 words) The performance of acid fuel cells operating at moderate temperatures ($\leq 250^{\circ}\text{C}$) is limited by the irreversibility of the O ₂ cathode. Much effort has been directed to identifying more active catalysts than highly dispersed platinum which sets the present bench mark. The optimization of the choice of electrolytes, however, also provides a way to speed up the kinetics. This paper lists various ways in which the electrolyte can influence the kinetics of the O ₂ reduction and discusses a few in more detail. The conclusion is reached that the adsorption of electrolyte components has a pronounced effect but that the kinetics do not have a strong dependence on pH or O ₂ solubility when mass transport control is not involved. Experimental results for a few new acid electrolytes and proton exchange membranes are presented.				
14. SUBJECT TERMS fuel cells operating on H ₂ and O ₂ in acid electrolyte; oxygen reduction kinetics; platinum electrocatalysts for O ₂ cathodes; new acids for H ₂ - O ₂ fuel cells			15. NUMBER OF PAGES 34	
			16. PRICE CODE	
17. SECURITY CLASSIFICATION OF REPORT Unclassified	18. SECURITY CLASSIFICATION OF THIS PAGE Unclassified	19. SECURITY CLASSIFICATION OF ABSTRACT Unclassified	20. LIMITATION OF ABSTRACT UL	

THE ELECTROLYTE FACTOR IN O₂ REDUCTION ELECTROCATALYSIS

by

E. Yeager, M. Razaq*, D. Gervasio, A. Razaq and D. Tryk
Case Center for Electrochemical Sciences
and the Chemistry Department
Case Western Reserve University
Cleveland, Ohio 44106

or	
Unannounced Justification	
By _____	
Distribution /	
Availability Codes	
Dist	Avail and/or Special
A-1	

ABSTRACT

The performance of acid fuel cells operating at moderate temperatures ($\leq 250^\circ\text{C}$) is limited by the irreversibility of the O₂ cathode. Much effort has been directed to identifying more active catalysts than highly dispersed platinum which sets the present bench mark. The optimization of the choice of electrolytes, however, also provides a way to speed up the kinetics. This paper lists various ways in which the electrolyte can influence the kinetics of the O₂ reduction and discusses a few in more detail. The conclusion is reached that the adsorption of electrolyte components has a pronounced effect but that the kinetics do not have a strong dependence on pH or O₂ solubility when mass transport control is not involved. Experimental results for a few new acid electrolytes and proton exchange membranes are presented.

I. INTRODUCTION

With fuel cells and metal-air batteries operating at low and moderate temperatures (i.e., $T \leq 250^\circ\text{C}$), the cell voltage is usually much lower than the thermodynamically expected value principally as the result of the irreversibility of the O₂ reduction reaction. Much effort has been directed to the search for more active catalysts than high area platinum, which sets the present bench mark. The optimization of the properties of the electrolyte phase, however, also provides a way to speed up the O₂ reduction kinetics. These properties include the following:

The electrolyte can influence the pathway and O₂ reduction kinetics through the following factors:

1. Activity coefficients of the reactants, intermediates and the transition state

*Present Address: Teledyne Analytical Instruments, 16830 Chestnut Street, City of Industry, California 91749-1580

2. Acidity
3. Competition between O_2 in solution and other electrolyte components for adsorption sites on the catalyst; blockage of sites for O_2 reduction by the adsorption of other electrolyte components
4. Dielectric properties of the electrolyte side of the interface
5. Double layer effects
6. Reorganizational free energy of activation; inner and outer sphere contributions
7. Solubilities of sparingly soluble reactants, intermediates and products (including gases)

Some of these factors are difficult to differentiate from each other in experimental studies. Of these factors the third (blockage of catalyst sites by adsorbed electrolyte components) is particularly important in explaining the substantial differences in the performance of platinum as a catalyst for O_2 reduction in various electrolytic solutions.

A quantitative discussion of the role of these electrolyte factors is limited by the uncertainty that still persists concerning the mechanism for the 4-electron reduction of O_2 to H_2O and OH^- in acid and alkaline electrolytes, respectively. Even so, the consideration of these factors provides a guide to the identification of new electrolytes which are more effective in promoting high catalytic activity with existing catalysts such as Pt, the transition metal macrocycle catalysts and the pyrochlores.

II. BACKGROUND

A. Mechanistic Considerations

Before proposing specific mechanisms, attention is called to three rather unusual features of the kinetics for the 4-electron O_2 reduction on Pt:

1. Measurements in the authors' laboratory indicate that the Tafel slope on bright polycrystalline Pt in the double layer region is almost independent of temperature over the range 25 to 250°C in concentrated H_3PO_4 and hence the apparent transfer coefficient α is approximately proportional to the absolute temperature over this range (1) (see Fig. 1).
2. The rates of O_2 reduction on Pt in a concentrated non-adsorbing acid solution (e.g., $HClO_4$) and concentrated alkaline solution (e.g., KOH) are within one order of magnitude of each other even though the hydrogen ion activity differs by a factor of 10^{-16} .
3. Hydrogen-deuterium isotopic studies (5) of O_2 reduction on Pt in 85% H_3PO_4 and D_3PO_4 do not indicate any kinetic isotope effect and this also implies that the rate determining step does not involve proton transfer.

On the other hand, Sepa, Voinovic and Damjanovic (6) have reported a value of $(\partial E_{\text{NHE}}/\partial \text{pH})_i = -0.12$ V for the potential range 0.85 to 0.70 V vs. NHE for O_2 reduction on Pt in 0.1 M H_2SO_4 . The bisulfate anion, however, is strongly adsorbed on Pt (4), and this can complicate the evaluation of the pH dependence of the kinetics in H_2SO_4 solutions. In 0.1 M KOH, these authors report $(\partial E_{\text{NHE}}/\partial \text{pH})_i = 0$.

The observation of a substantial temperature dependence for α is not unique to the O_2 reduction reaction and includes hydrogen overpotential on various metals, even Hg (7). Various factors which may contribute to a temperature dependent apparent transfer coefficient have been discussed by Conway (7) but just why the effect is so large for such electrode processes as H_2 generation and O_2 reduction in acid electrolytes remains to be explained. One possibility is that the rate determining step does not involve a charge transfer process but rather the adsorption of a neutral species such as O_2 itself. Under such circumstances the potential dependence may be associated principally with an entropy of activation and its dependence on the potential gradient across the interface. This can result in an apparent value of α which is proportional to the absolute temperature (7), as is further discussed later in this paper.

Scharifker et al. (8) also have examined the reduction of O_2 on Pt in concentrated H_3PO_4 at high temperatures and have concluded that the Tafel slope is proportional to the absolute temperature for O_2 reduction in concentrated H_3PO_4 . They propose that impurity effects cause the temperature dependence of the transfer coefficient α . The measurements of Scharifker et al. were made with microelectrodes and are subject to various problems such as leakage current. The studies in our laboratory have used the rotating disk technique.

Impurity effects can yield erroneous Tafel slopes but it is very unlikely that the Tafel slope would be -0.120 V/decade or $-2RT/f$ over a temperature range of 25 to 250°C . The value at 25°C reported by most researchers is -0.12 V/decade at 25°C and not the value of -0.09 V/decade obtained by Scharifker et al. Further work is required to resolve this question.

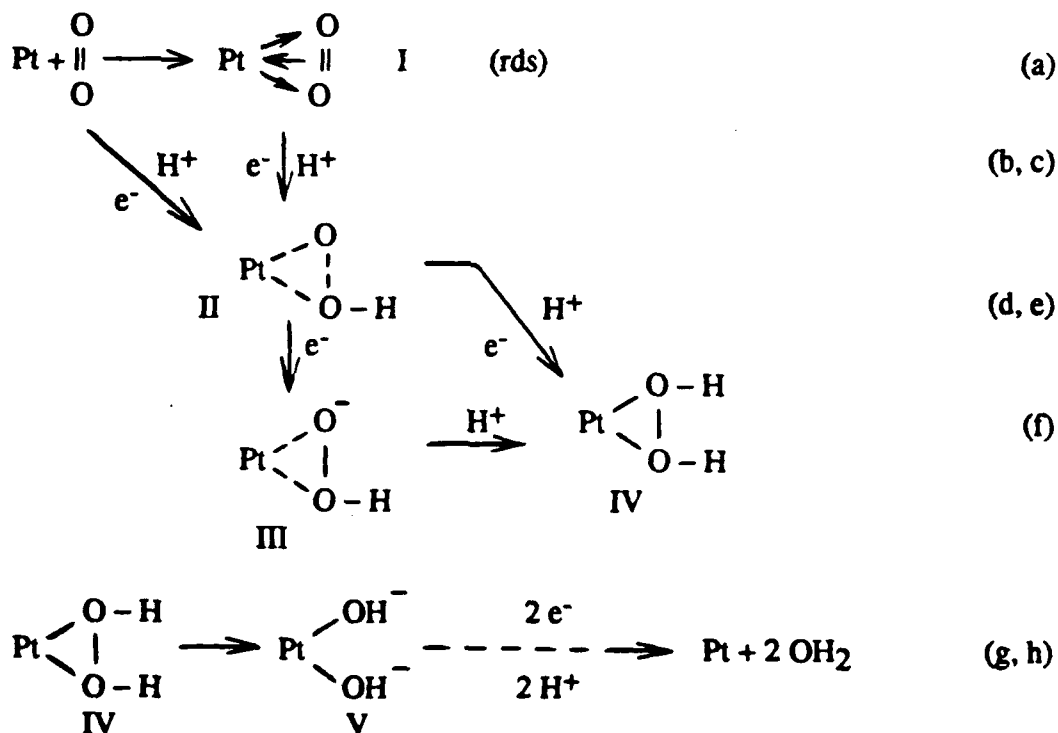
In order to illustrate the electrolyte effects listed earlier in this paper, consider the Mechanism I for O_2 reduction on Pt in acid electrolytes. Species I involves a lateral interaction of the π -orbitals of the O_2 with empty d_{z^2} orbitals of a surface platinum atom with back bonding from the partially filled d_{xz} or d_{yz} orbitals of the Pt to the π^* orbitals of the O_2 . The formation of a strong metal - oxygen interaction will result in a weakening of the O-O bond and an increase in its length. The surface species II corresponds to the superoxide while III and IV are peroxides. The O_2 reduction is proposed to proceed by reaction (a) rather than (b) and with reaction (a) rate determining. Reaction (h) corresponds to the reduction of PtOH and would be expected to proceed through multiple steps.

With reaction (a) rate determining, the rate of the forward process can be given by

$$v_f = \frac{k_f}{\gamma_{\ddagger}} \cdot a_{O_2} \cdot a_{Pt} \quad [1]$$

where k_f is the forward rate constant, γ_{\ddagger} is the activity coefficient for the transition state, a_{O_2} is the activity of O_2 in the electrolyte phase and a_{Pt} is the activity of bare Pt sites. The interaction of water with the Pt sites is assumed to be weak.

Mechanism I for O_2 Reduction



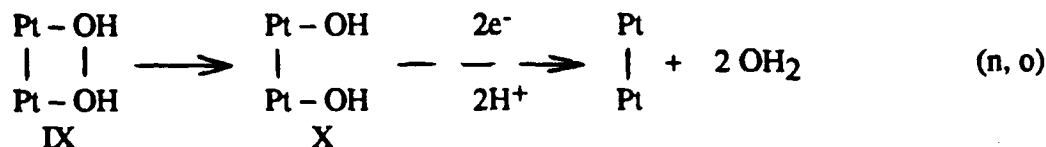
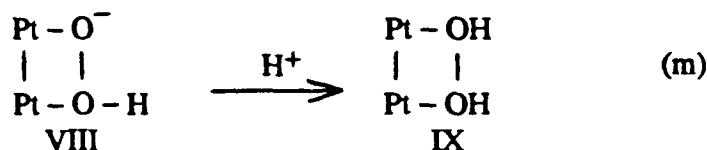
II. The corresponding reactions for a dual site mechanism are given in Mechanism

The corresponding kinetic equation is

$$v_f = \frac{k_f}{\gamma_{\ddagger}} \cdot a_{O_2} \cdot a_{Pt-Pt} \quad [2]$$

where $(a_{\text{Pt-Pt}})$ corresponds to the probability of having two adjacent unoccupied Pt sites with the proper geometry and electron orbitals for the chemisorption of O_2 .

Mechanism II for O_2 Reduction (dual site)



B. Oxygen Solubility

The activity of O_2 in the electrolyte phase is controlled by the condition that the chemical potential of the dissolved O_2 be equal to that of the O_2 in the gas phase in equilibrium with the electrolyte phase; i.e.,

$$(\mu_{\text{O}_2})_{\text{g}} = (\mu_{\text{O}_2}^0)_{\text{g}} + RT \ln(a_{\text{O}_2})_{\text{g}} = (\mu_{\text{O}_2})_{\text{el}} = (\mu_{\text{O}_2}^0)_{\text{el}} + RT \ln(a_{\text{O}_2})_{\text{el}} \quad [3]$$

where the μ terms correspond to the chemical potentials of the subscripted species, the a terms are the activities and the μ^0 terms correspond to the standard state values. Thus the chemical potential of the O_2 in the electrolyte phase is independent of the particular electrolyte phase provided the O_2 in the electrolyte phase is in equilibrium with the gas phase. The O_2 solubility should not directly influence the kinetics unless the reaction is under transport control in the gas and/or electrolyte phases. This can be seen by recalling from absolute rate theory (29) that the rate constant k_f in eq. 1 is given by

$$k_f = \frac{xkT}{h} K_{\ddagger} = \frac{xkT}{h} \cdot \exp - \frac{(\mu_{\ddagger}^0) - (\mu_{O_2}^0)_{el} - (\mu_{Pt}^0)}{RT} \quad [4]$$

where x is the transmission factor, K_{\ddagger} is the apparent equilibrium constant for the $(O-O)_{ads}$ reactant in the transition state (\ddagger), μ_{\ddagger}^0 is the chemical potential of the adsorbed oxygen in the transition state and the remaining symbols have their usual meaning. Recall that the equilibrium constant and chemical potential for the transition state are calculated from the partition functions with the vibration mode corresponding to transmission over the potential energy barrier omitted since it has already been used to derive the pre-exponential term xkT/h . Combining eqs. 1 and 4 yields

$$v_f = \frac{xkT}{\gamma_{\ddagger} h} \cdot \exp - \frac{(\mu_{\ddagger}^0) - (\mu_{O_2}^0)_{el} - (\mu_{Pt}^0)}{RT} \cdot (a_{O_2})_{el} (a_{Pt}) \quad [5]$$

or

$$v_f = \frac{xkT}{\gamma_{\ddagger} h} \cdot \exp - \frac{(\mu_{\ddagger}^0)}{RT} \cdot \exp \frac{(\mu_{O_2})_g}{RT} \cdot \exp \frac{(\mu_{Pt})}{RT} \quad [5a]$$

with $(\mu_{O_2})_g = (\mu_{O_2})_{el} = \text{constant}$. A similar equation to 5a can be written, based on eq. 2 with reaction (i) rate determining. The dependence of the kinetics on the factor $(a_{O_2})_{el}$ is offset by the term $\exp (\mu_{O_2})_{el}/RT$ since $(\mu_{O_2})_g$ is held constant. The solubility of O_2 in the particular electrolytic solution has no direct effect on any term in eq. 5a but in a sense it may have a small indirect effect on the standard state chemical potential (μ_{\ddagger}^0) of the $O-O$ species involved in the transition state. The interaction with the electrolytic solution in the transition state may have some similarity with the interaction of dissolved O_2 with the electrolytic solution. This effect would be expected to be quite small compared with that involving the change in the activity of the "bare" Pt (μ_{Pt}) in eq. 5a, particularly when specific adsorption of the electrolyte occurs on Pt. In general O_2 solubility has a substantial effect on the polarization curve for O_2 electroreduction only when mass transport of O_2 is controlling. Thus, it is not surprising that the solubility of O_2 drops off by a factor of 10^{-2} between 0.1 and 10 M KOH without a corresponding drop-off in the rate of O_2 reduction on Pt electrodes in concentrated KOH. Of course, for a given electrolyte-solvent system, the rate of adsorption of O_2 (e.g., reaction a) is proportional to the O_2 concentration with $(\mu_{O_2})_{el}$ constant (see eq. 5).

C. Activity Coefficient for the Transition State

According to absolute rate theory, the activity coefficient of the transition state γ_{\ddagger} can have a major effect on the rate of the electrode reaction and is expected to be a function of the electrolyte and solvent as well as the electrode potential. For example, the coadsorption of OH^- or other ions of the electrolyte should have a substantial effect on γ_{\ddagger} for the transition states for reactions (a) and (i) in addition to blocking sites. Since the adsorption of ions is potential dependent, this will result in an additional potential dependent term in the rate equations through γ_{\ddagger} and therefore will perturb the Tafel slope dependence on temperature (see also ref. 24).

D. Tafel Slope and Entropies of Activation

The Tafel slope b is related to the standard free energy of activation $(\Delta G_{\ddagger})^0$ by the equation (see e.g., ref. 7)

$$\frac{1}{b} = \left(\frac{\partial \ln i}{\partial E} \right)_T = - \left(\frac{\partial (\Delta G_{\ddagger})^0 / RT}{\partial E} \right)_T = - \frac{\partial}{\partial E} \left(\frac{(\Delta H_{\ddagger})^0 - T(\Delta S_{\ddagger})^0 + \beta f E}{RT} \right)_T \quad [6]$$

where $(\Delta H_{\ddagger})^0$ and $(\Delta S_{\ddagger})^0$ are the standard enthalpy and standard entropy of activation. If $(\Delta H_{\ddagger})^0$ and β are taken as independent of potential, this equation reduces to

$$\left(\frac{\partial \ln i}{\partial E} \right)_T = - (\beta + cT) f / (RT) \quad [7]$$

where

$$c = - \left(\frac{\partial (\Delta S_{\ddagger})^0 / f}{\partial E} \right)_T \quad [8]$$

and

$$b = -RT/[f(\beta + cT)] = -RT/\alpha f \quad [9]$$

where α is the apparent transfer coefficient.

Experimental data (1,2) obtained in the authors' laboratory for O_2 reduction in concentrated H_3PO_4 over the temperature range 25 to 250°C on a Pt rotating disk electrode yield an apparent transfer coefficient α of the form

$$\alpha = a + cT \quad [10]$$

with $a = 0.08$ and $c = 0.0014 = ^\circ K^{-1}$. Therefore, at room temperature and above, $\alpha = cT$ and $\beta < 1/2$. Thus most of the potential dependence of the reaction rate appears to be associated with the potential dependence of the entropy of activation rather than the simple change of the height of the potential energy barrier. For a rate determining step involving the adsorption of a neutral species such as O_2 , the potential dependence of the entropy of activation may be the principal source of the potential dependence of the reaction rate. The fact that the apparent transfer coefficient is 0.5 at 298°K, however, would need to be explained.

The source of the anomalous temperature dependence of the Tafel slope for O_2 and other electrocatalytic reactions remains uncertain. This situation makes it difficult to interpret the kinetic data for such reactions and warrants urgent attention.

E. Competition of O_2 with Electrolyte Components for Adsorption Sites

While water is important to the O_2 reduction reaction, the adsorption of H_2O or other polar species in the electrolytic solution may lead to a reduction in the accessibility of O_2 to the transition metal sites of the catalyst and hence a depression of the kinetics. There is little doubt that the adsorption of such species as HSO_4^- , Cl^- and $H_2PO_4^-$ depresses the kinetics of O_2 reduction on platinum.

One way to bias the situation to preferentially favor O_2 over other much more polar species is to impose steric restrictions. For example, Collman and Anson (3,4) have reported that the face-to-face Co-Co porphyrin (Fig. 2) has high catalytic activity for the 4-electron reduction of O_2 to H_2O in acid electrolytes when the Co-Co distance is $\sim 4.0 \text{ \AA}$ which corresponds to that expected for a di-oxygen bridge. Further research by these workers, however, has revealed that the 4-electron reduction is also catalyzed by the corresponding Co-Al complex and the Co- $2H^+$ complex with the same distance between the two metal centers or the equivalent distance in the Co- $2H^+$ form. A likely explanation is that the cavity fits O_2 but not the larger acid anions, thus favoring O_2 adsorption between the two face-to-face porphyrin groups. Furthermore, the dielectric constant seen by the species within this cavity is considerably lower than in the bulk of the electrolytic solution. The environment within the cavity becomes more favorable for

non-polar O_2 and less favorable for the water molecules. This may be considered the equivalent of a "dry cave" effect. Another possibility is that Lewis or Bronsted acid in the second site within the diporphyrin plays a beneficial role in the O_2 4-electron reduction.

The dry cave concept may also be applicable to platinum electrodes. One way of rendering Pt sites more favorable for O_2 adsorption is to form a self assembling weakly adsorbed ordered layer of a surfactant-type molecule at the electrode surface. For example, the additive $C_4F_9-SO_2-NH-SO_2-CF_3$, prepared by DesMarteau and Singh (13), at a concentration of 0.5% by weight in 85% H_3PO_4 decreases the O_2 overpotential with a Prototech platinum catalyzed electrode by ~50 mV. Water must still have access to the surface of the catalyst as is the case with a short fluorocarbon tail. It is not so much that the surfactant reduces the free energy of adsorption of the O_2 but rather that it increases the free energy of adsorption of H_2O and ionic components because of the lower effective dielectric constant in the electrolyte phase immediately adjacent to the catalyst surface.

An alternative to the adsorption of O_2 , particularly in concentrated alkaline electrolytes, is to reduce the O_2 to the superoxide state ($O_2^{\cdot -}$) by an outer sphere one-electron transfer. The relatively polar superoxide ion can then be adsorbed on the catalyst sites and undergo reaction (b) to (h) or (j) to (o), yielding a total of 4 electrons per O_2 .

III. EXPERIMENTAL STUDIES OF O_2 REDUCTION IN VARIOUS ACID ELECTROLYTES

The authors have examined the performance of gas diffusion O_2 cathodes using highly dispersed Pt in a number of concentrated purified acid electrolytes including perfluorosulfonic, phosphonic, sulfonimide and carboxylic acids, which were synthesized by Prof. Darryl DesMarteau of Clemson University and Prof. Donald Burton of the University of Iowa. The O_2 cathode has substantially lower polarization in some of these electrolytes, principally because they are not strongly adsorbed on the high area Pt catalyst. The perfluoroacids usually have order of magnitude higher O_2 solubilities than 85% H_3PO_4 but this is not expected to have a large direct effect on the O_2 reduction kinetics for the reasons discussed earlier. The solubility, however, can play an important role when mass transport control is involved. The diffusion coefficients must also be taken into account; they tend to be comparable to or higher in the perfluorinated acids than in H_3PO_4 at comparable high concentrations.

Of the various strong acids, $CF_3SO_3H \cdot x H_2O$ would normally be among the most attractive in terms of low overpotentials, lack of specific adsorption on Pt, high O_2 solubility and the know-how to clean this acid up with respect to adsorbable impurities. Unfortunately the perfluorosulfonic acids have much lower ionic conductivity by a factor of 10^{-4} fold than H_3PO_4 at high concentrations and this leads to excessive ohmic loss that may more than offset the lower polarization at the air cathodes for fuel cells using this electrolyte.

A. Mixtures of Concentrated Phosphoric and Trifluoromethane Sulfonic Acids (9,10)

An alternative approach is the use of a mixture of H_3PO_4 with a strong acid such as $\text{CF}_3\text{SO}_3\text{H}$ with both acids at high concentrations, e.g., 25 mol % of each acid and 50 mol% H_2O . The adsorption of the phosphate anion on the Pt surface can still occur but the activity of the phosphoric acid should be significantly depressed and this should reduce the adsorption of the phosphate anion on the Pt surface. The solubility of O_2 would still be increased although not by as much as with the pure $\text{CF}_3\text{SO}_3\text{H}$. The presence of the H_3PO_4 is expected to keep the conductivity of the electrolyte still quite high.

Prior work using laser Raman spectroscopy (9) has demonstrated that in the $\text{CF}_3\text{SO}_3\text{H} - \text{H}_3\text{PO}_4 - \text{H}_2\text{O}$ system, the sulfonic acid is almost fully ionized and protonates both H_2O and H_3PO_4 for mole fractions of the sulfonic acid less than 0.4. Furthermore, these spectroscopic studies indicate that the formation of either the proton monohydrate (H_3O^+) or the phosphonium ion [$\text{P}(\text{OH})_4^+$] is sufficient to promote the ionization of the $\text{CF}_3\text{SO}_3\text{H}$; i.e.,

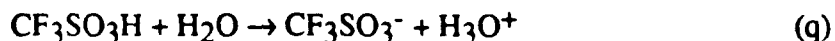


Figure 3 indicates the Tafel plots for O_2 reduction on smooth polycrystalline Pt (10) in the $\text{CF}_3\text{SO}_3\text{H} - \text{H}_3\text{PO}_4 - \text{H}_2\text{O}$ mixtures and in 86% H_3PO_4 at 25°C . The measurements were made with the rotating disk technique; details are given elsewhere (10). The abscissa corresponds to the current density i corrected for mass transport by multiplication by the factor $i_d/(i_d - i)$ where i_d is the diffusion limiting current density. For Fig. 3, the rotation rate was 1600 rpm. The Tafel slope in the potential region 0.9 to 0.7 V was ~ -0.12 V/decade which at 25°C corresponds to $-2RT/f$. The bending of the Tafel plot at more positive potentials is due to the initial stages of the anodic film (PtOH) formation on Pt. The deviations from linearity in the Tafel plots at low potential may be due to a slight error in the i_d values used in constructing this figure. These were obtained from the slopes of the Koutecky - Levich plots of $1/i$ vs. $1/\omega^{1/2}$. As i approaches i_d , any error in i_d is greatly magnified. Another possibility is a kinetic limiting current associated with a step which is potential independent or which has only a very small potential dependence; e.g., the dissociative desorption of O_2 .

The reaction order with respect to O_2 has been confirmed as first order from the slope of plots of $\log i$ vs. $\log [(i_d - i)/i_d]$ obtained with the rotating disk electrode (10). For example, for the 30 mol% H_3PO_4 - 20 mol% TFMSA - 50% H_2O solution, the slopes of these linear plots varied from 1.06 at 0.70 V to 1.1 at 0.55 V. No change in Tafel slope was obtained in going from 86% H_3PO_4 to 25% mol% TFMSA - 25% H_3PO_4 - 50% H_2O .

The Tafel slope of -0.12 V/decade would ordinarily be taken as evidence that the rate determining step for O₂ reduction on Pt is the first electron transfer step. The unexpected temperature independence of the Tafel slope, discussed earlier, however, raises questions concerning the significance of the Tafel slopes, at least for multistep electrode reactions involving adsorbed intermediates.

The first order rate constant is defined by the rate equation written in the form

$$i = 4 f k P_{O_2} \cdot (i_d - i)/(i_d) \quad [11]$$

where P_{O_2} is the partial pressure (atm) of O₂ gas in equilibrium with the electrolytic solution. In Table 1 are listed the ratios of the rate constants (k_2) for the mixed acids to that (k_1) of the 86% H₃PO₄, both at 0.80 V vs. RHE. The ratios of the rate constants were calculated using the following equation:

$$\frac{k_2}{k_1} = \left(\frac{i_d - i}{i i_d} \right)_1 \cdot \left(\frac{i i_d}{i_d - i} \right)_2 \quad [12]$$

with the condition that P_{O_2} and the potential are the same for both electrolytes.

The exchange current densities varied from 1.7×10^{-8} A/cm² for 86% H₃PO₄ to 7.5×10^{-8} A/cm² for the mixture with the highest TFMSA concentration, 25 mol% H₃PO₄ - 25 mol% TFMSA - 50 mol% H₂O at 25°C. The corresponding change in the ratio of the rate constants is $k_2/k_1 = 5.9$ at $E = 0.80$ V vs. RHE (see Table 1). In this comparison, the number of electrons per O₂ molecule has been taken to be 4.0 and to be the same for all of the measurements corresponding to the linear region in the Tafel plots.

The k_2/k_1 ratios are close to unity for the acid mixtures with up to 12.5 mol% TFMSA but deviate substantially from unity for higher mol% of TFMSA (see Table 1). Several factors can contribute to the change of the k_2/k_1 ratio including changes in the activity coefficient in the transition state, the activities of H₂O and the partially solvated protons and the adsorption of phosphate species on the Pt surface. Impurity effects can not be discarded as a possible factor contributing to the change of the k_2/k_1 ratio at high H₃PO₄ and TFMSA concentration since these acids are difficult to purify to the extent that the Pt surface is completely free of impurities. The faster kinetics in the concentrated CF₃SO₃H solution in Table 1 and Fig. 3 may be caused by a decrease in the adsorption of the H₂PO₄⁻ on the Pt surface and/or the increased solubility of O₂ in the concentrated CF₃SO₃H compared with 86% H₃PO₄. The latter seems unlikely for the reasons discussed earlier.

The results on smooth Pt suggest that the addition of a strong acid to concentrated H₃PO₄ will lower the polarization for O₂ reduction on high performance gas-fed O₂ cathodes using highly dispersed Pt as the catalyst in phosphoric acid fuel cells. TFMSA,

however, is not attractive as an additive in fuel cells operating at temperatures of $\sim 190^\circ\text{C}$ because of its volatility. The addition of TFMSA to concentrated H_3PO_4 also decreases the conductivity. In concentrated H_3PO_4 , extensive hydrogen bonding occurs and the conduction is principally by a Grotthus-type conduction mechanism involving protons hopping between adjacent H_3PO_4 molecules (see Fig. 4). The TFMSA reduces the intermolecular hydrogen bonding and thus reduces the conductivity. The increased ohmic loss is likely to offset much of the gain in cell voltage associated with the decrease in polarization of the O_2 cathode.

Furthermore, $\text{CF}_3\text{SO}_3\text{H}$ wets Teflon (11) in gas-fed electrodes at high concentrations ($> 6\text{M}$) and this results in the flooding of the Teflon bonded gas diffusion electrodes used in acid fuel cells.

B. O_2 Reduction with Perfluorinated Sulfonyl Imide as an Additive to Concentrated H_3PO_4

Some of the perfluorinated phosphoric, phosphonic, sulfonyl imide and carboxylic electrolytes which have been investigated by the authors have substantial effects on the O_2 electrode polarization even when added at relatively low concentrations to 85% H_3PO_4 (12, 13) (see Table 2).

Of particular interest are the perfluorosulfonimides (PFSI), such as the acid $\text{CF}_3\text{SO}_2\text{N}(\text{H})\text{SO}_2\text{C}_4\text{F}_9$. The voltammetry curves for Pt in N_2 saturated 85% H_3PO_4 with and without 4% (0.16M) of this PFSI are shown in Fig. 5. The addition of the PFSI has relatively little effect on the voltammetry curve for Pt in 85% H_3PO_4 without O_2 present. This voltammogram plus others for more dilute solutions of PFSI in H_3PO_4 provide evidence that the PFSI is not strongly adsorbed on Pt while H_2PO_4^- is strongly adsorbed. Figure 6 presents the polarization curve recorded with the rotating disk electrode technique. The polarization curves for the 85% H_3PO_4 with and without 4% PFSI (Fig. 6) indicate that PFSI lowers the half wave potential $E_{1/2}$ by $\sim 90\text{ mV}$ while the limiting current is increased by $\sim 64\%$.

The mixture of 85% H_3PO_4 and 4% PFSI has the milky appearance of an emulsion. At high concentrations H_3PO_4 solutions involve a three-dimensional strongly hydrogen bonded structure and the PFSI tends to be squeezed out of the bulk H_3PO_4 solution forming a physically adsorbed layer at the electrode surface with the hydrocarbon C_4F_9 tail probably oriented towards the electrode surface and the polar end towards the bulk solution. The structure of this layer including its thickness needs to be established. *In-situ* spectroscopic techniques such as infrared reflectance (SNIFTIRS, EMIRS) and Raman (SERS) should be able to provide such information.

The physically adsorbed PFSI layer at the electrode surface will perturb the structure of the double layer and lower the effective dielectric constant adjacent to the electrode surface. The chemical potentials of adsorbed ionic species as well as H_3PO_4 and water molecules are dependent on the dielectric properties in the electrolyte phase immediately adjacent the Pt electrode. As discussed earlier the O_2 molecule is relatively

non-polar and the decrease in dielectric constant is expected to favor O_2 adsorption, not so much because of a direct interaction with the $(O_2)_{ads}$ but rather through the destabilization of adsorbed more polar species and the freeing up of more adsorption sites for O_2 . The PFSI layer is probably only a single molecule thick and does not seem to interfere with O_2 and water/proton transport at this interface. This layer resembles a self-ordered Langmuir-Blodgett film with the fluorocarbon end towards the platinum. In this layer O_2 has a higher concentration than in the bulk H_3PO_4 and H_2O has a lower concentration (13).

The PFSI is a relatively strong acid ($pK_a = 0.91$) compared with the first ionization of H_3PO_4 ($pK_{a-1} = 2.15$). The solubility of the PFSI in 85% H_3PO_4 , however, is slightly less than 0.5% and the PFSI in excess of 0.5% forms an emulsion. The addition of 4% PFSI would suppress the ionization of the H_3PO_4 but the hydrogen ion concentration would change by only a small amount (less than 1%).

The generation of H_2O_2 was monitored with the rotating ring-disk technique with a potential of 1.1 V vs. RHE applied to the ring while scanning the disk potential from 1.0 to 0.40 V. The ratio of the peroxide oxidation current on the ring electrode to the O_2 reduction current on the disk was very small and essentially the same with and without the 4% PFSI. In Fig. 6 the increase in the diffusion limiting current density in the rotating disk experiment with 4% PFSI added to 85% H_3PO_4 is relatively large (64% at 2500 rpm) and depends on the change in O_2 solubility and diffusion coefficients of the O_2 in the electrolytic solution. These were determined using the microelectrode technique (14). The solubility and diffusion coefficients are given in Table 3. Both O_2 solubility and diffusion coefficients are much larger in the 84% PFSI than the 85% H_3PO_4 . The difference in the $CD^{2/3}$ product for the 85% H_3PO_4 and 84% PFSI is sufficient to account for the 64% increase in limiting current density with 4% PFSI added to 85% H_3PO_4 .

The polarization of the O_2 cathode (Fig. 7) has also been examined using high surface area Prototech gas-fed electrodes in 85% H_3PO_4 without and with 0.5% PFSI at 70°C in a micro H_2/O_2 fuel cell (Fig. 8). The polarization is 70 mV less at a current density of 100 mA/cm² in the 0.5% PFSI solution. The polarization curves in the 0.5% PFSI + 85% H_3PO_4 solutions are independent of time over the 48 h time period of the experiments. This suggests that in the mixed electrolyte the concentration of PFSI is lower than the critical value which would promote flooding of the gas-fed electrodes. At lower concentrations (e.g., 0.126%) the PFSI still depresses the polarization at 70°C but not by as much (~30 mV at 100 mA/cm²).

The volatility of the PFSI in 85% H_3PO_4 at 150°C was checked by heating the mixture in a beaker. After 5h with 4% PFSI + 85% H_3PO_4 , a substantial amount of the PFSI was lost by evaporation. Thus the intrinsic vapor pressure of the PFSI itself is too high for operations under acid fuel cell conditions (190°C). A condenser system could be used to recover the PFSI from the vapor phase. Work is in process to develop additives of this type with lower vapor pressure as a cooperative effort with Professors D. DesMarteau of Clemson University and D. Burton of the University of Iowa.

Other electrolytes which have been investigated in the authors' laboratory at both low and high concentrations with Prototech high area Pt electrodes are listed in Table 2 for either 70 or 100°C together with polarization data. The relatively poor performance of the 84% (FSO₂)₂ NH may be due to stability problems and/or impurities. The perfluorosulfonic carboacid probably forms a self-assembled layer with the C₄F₉ tail closest to the interface.

C. O₂ Reduction In Concentrated Perfluoro Bis Phosphoric Acid

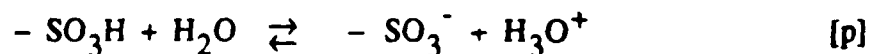
The decrease in polarization for the Prototech Pt catalyzed O₂ carbon in 85% (HO)₂OP-CF₂-CF₂-PO (OH)₂ as compared with 85% H₃PO₄ is quite substantial at 100°C (see Table 2). These electrodes have been operated in this electrolyte at 200°C with relatively little increase in polarization over 500h. The bis phosphoric acids were synthesized by Prof. D. Burton and his research group (27).

IV. POLYMER ELECTROLYTES

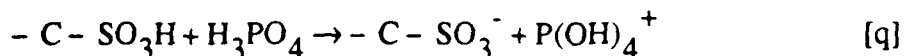
A. The duPont Nafion and Dow 560 Cation Exchange Polymers

The perfluorosulfonic acid cation exchange polymer(Nafion) (Fig. 9) has been used as the electrolyte in the proton exchange membrane (PEM) H₂/O₂ fuel cell. (For a recent review of the PEM fuel cell systems, see ref. 26.) Similar sulfonic acid ionomers have been developed by Dow Chemical with lower equivalent weights (e.g., 560) than that (1100) of duPont Nafion. The lower equivalent weight polymers of Dow have higher conductivity. The performance of the gas-fed Pt catalyzed O₂ cathodes is surprisingly good even at very high current densities (several A/cm²) principally because the cation exchange polymer electrolyte is not strongly adsorbed on the Pt in contrast to concentrated H₃PO₄. (Care must be taken to remove impurities in the SPE such as H₂PO₄⁻, HSO₄⁻, Cl⁻ which adsorb on Pt.) The operating temperature, however, is generally limited to ≤100°C. At higher temperatures the polymer becomes dehydrated and loses its conductivity as well as shrinks. The operating temperatures can be extended to somewhat higher values by pressurization of the cell but this adversely affects the overall efficiency of the fuel cell system. Furthermore, the tolerance of the Pt catalyzed H₂ anode to CO is very low (ppm) unless the operating temperature is at least 150°C. Even higher temperatures are desirable to utilize the heat from the fuel cell for the H₂ reformer. It is impractical to achieve such high temperatures by pressurization.

The ionization of the sulfonic acid groups in the polymer requires at least one water molecule per H⁺ produced by the ionization; i.e.,



groups are no longer ionized. The ionization of the SO_3H groups, however, can be produced by other Bronsted bases such as H_3PO_4 ; i.e.,



Reaction (q) has been verified using laser Raman in mixtures of $\text{CF}_3\text{SO}_3\text{H}$ with $\text{H}_3\text{PO}_4 + \text{H}_2\text{O}$. Figure 10 indicates the retention of the conductivity of a Nafion 117 membrane at 175°C over the time period of the experiment (60 h). The membrane was preequilibrated with H_3PO_4 by soaking it in 85% H_3PO_4 at 150°C for 12h. Platinum electrodes were pressed against each side of the membrane with a cross section of 2 cm^2 . With water equilibrated Nafion 117, the conductivity decays rapidly to a value far too low for fuel cell applications (see Fig. 11).

The use of H_3PO_4 to solvate protons in Nafion and similar ionomers has the disadvantage that the H_3PO_4 and its dissociation products are adsorbed on platinum and reduce its catalytic activity. The increase in the kinetics at the higher operating temperatures probably more than offsets the decrease arising from the adsorption of the phosphate. Nonetheless, it would be attractive to find an acid which would solvate the proton and have Grotthus conduction but not suppress the kinetics of the O_2 reduction. One promising approach is to bind into the polymer $-\text{PO}(\text{OH})_2$ groups. While these groups may be specifically adsorbed at the Pt - polymer interface, steric factors associated with the limited flexibility of the polymer should prevent the blockage of many of the Pt sites, thus leaving them available for the adsorption of O_2 .

B. Structural Features of the Perfluorosulfonic Acid Polymers

Gierke (15) has proposed that Nafion has a cluster-network structure of the type indicated in Fig. 12. The continuous phase involves the hydrophobic fluorocarbon backbone. The polymeric $-\text{SO}_3^-$ ions and any added electrolytes are in spherical clusters, which are interconnected by short narrow channels. The sulfonate anions are probably located principally at the interface between the electrolyte and the fluorocarbon backbone. The shaded areas are the equivalent of double layer regions with the negative charge of the ionized sulfonic acid groups compensated by hydronium ions (not shown). Anions from external sources are electrostatically repelled from these regions.

Verbrugge and Hill (16, 17) have used the model shown in Fig. 13 to account for the transport properties of the du Pont and the Dow ion exchange membranes. The pores have diameters of $\sim 40\text{\AA}$ on the basis of X-ray scattering (15). In the work of Verbrugge and Hill, the membranes were in contact with concentrated sulfuric acid and the co-ion in Fig. 13 is the bisulfate anion, HSO_4^- . With the Nafion equilibrated with 85% H_3PO_4 (Fig. 10) the aqueous phase in Fig. 13 is principally concentrated H_3PO_4 . From various transport experiments (16-18), Verbrugge and Hill concluded that proton transfer is faster in the Dow 560 polymer than in the duPont Nafion 117 and the Dow polymers have lower permeability than the Nafion 117.

C. Gas Diffusion Electrodes with Solid Polymer Exchange Ionomers as the Ionic Conducting Phase

The structure of the gas diffusion SPE electrodes is highly dependent on the procedures used in their fabrication. In the authors' laboratory use has been made of gas diffusion electrodes with Teflon (duPont T-30B emulsions) or Fluon (Imperial Chemical Industries, Ltd.) as a binding and wet proofing agent and with highly dispersed Pt particles (15 -20Å diameter) on a high area carbon support (e.g., steam activated Shawinigan black). In some instances, these electrodes have been pressed against the Nafion membrane. It is unlikely under these conditions, however, that the polymer is in direct contact with a large fraction of the catalyst particles. Rather, residual liquid electrolyte from within the polymer is in contact with the catalyst and completes the ionic circuit between the ionic conducting polymer and the catalyst particles. The long term stability of such an arrangement is in question, particularly at higher temperatures.

A more promising arrangement is to blend the duPont Nafion or Dow 560 polymer into the active catalyst layer with the solid ionomer replacing the fluid electrolyte which in a properly designed gas diffusion electrode is in contact with most of the dispersed Pt catalyst particles. The fabrication of such an electrode, however, is more an art than a science. The ionomer is added in solution form to a slurry consisting of dispersed Pt on a carbon support together with Fluon. This binder is preferred to Teflon because the Fluon does not require the high temperature (375°C) needed to decompose or sublime out the surfactant (duPont Triton X-100), from the Teflon bonded electrodes (19). The excess water is removed from the slurry by suction filtration and a thin layer (e.g., 0.01 cm) bonded to a carbon backing paper.

The model (Fig. 14) which has been used is similar to that proposed by Giner and Hunter (17). The gas is fed into the active catalyzed layer through hydrophobic channels consisting of Fluon. The effective radius of channels is less than the mean free path in the gas at 1 atm; therefore, Knudsen diffusion is involved. The reacting gas then enters the flooded agglomerates and diffuses through the electrolyte phase to the dispersed catalysts. With highly dispersed Pt on a high area carbon support, the Pt particles in most instances are expected to be single crystals with each acting like a microelectrode with greatly enhanced transport to and from the Pt surface (21). Some of the Fluon is also incorporated into the Pt-catalyzed carbon-electrolyte agglomerates to bind them together but these regions are hydrophilic.

Electrodes of this type can operate on pure O₂ or air at current densities of several A/cm² either in contact with a bulk fluid electrolyte such as concentrated H₃PO₄ or in a solid polymer electrolyte cell where the anolyte and catholyte are both solid ionomers. The use of such solid ionomer loaded O₂ electrodes in fluid electrolytes may have several advantages; e.g.,

1. long term localization of the electrolyte phase within the porous catalyzed active layer and hence longer life;

2. much higher O_2 solubility than in concentrated electrolytes such as H_3PO_4 , which facilitates mass transport at higher current densities;
3. prevention of gas blow-through in electrodes when operating with excess gas pressure over that on the electrolyte side;
4. retention of adsorbed transition macrocycle catalysts on high area carbon supports without the need for high temperature treatment.

The stabilization of adsorbed transition metal macrocycle catalysts is illustrated in Fig. 15 for an O_2 cathode with cobalt tetramethoxyphenyl porphyrin (CoTMPP) adsorbed on a steam activated Shawinigan black using Fluon as the binding agent and with and without Nafion 117 in the active catalyst layer in 85% H_3PO_4 at an operating temperature of 100°C. The catalytic activity of the CoTMPP is not retained even for sufficient time for the polarization measurements without heat treatment at $\geq 600^\circ C$ in the absence of the Nafion ionomer in the active layer. It is hoped that long term stability of the macrocycle and other similar electrocatalysts adsorbed on high area carbon can be achieved without heat treatment at temperatures above 150°C. This will make it possible to optimize the macrocycle chemically by introduction of various functional groups which are normally destroyed during heat treatment.

The curvature in the Tafel plot with Nafion in Fig. 15 is probably caused by either residual ohmic losses in the active layer not completely corrected in the polarization measurements and/or mass transport problems. O_2 reduction with the CoTMPP catalyst proceeds via a peroxide (parallel) pathway in the acid electrolyte.

The platinum catalyzed gas diffusion O_2 cathodes with Nafion (117) as the ionic conductors in the active layer have polarization curves in 85% H_3PO_4 bulk solution with only minor differences at $T = 100^\circ C$ compared to the same type of electrodes made up without Nafion in 85% H_3PO_4 as the ionic conductor (Fig. 16). The potential of the Nafion loaded electrodes is 20 to 40 mV more positive. The deviation of these curves from Tafel linearity at high current densities is attributed principally to distributed ohmic losses in the active layer which could not be compensated or fully corrected in the polarization measurements.

The small difference with and without Nafion is not surprising since the polar phase of the Nafion is believed to be predominant at the Pt-Nafion interface.

Several factors may contribute to the slightly improved performance. These include

- less initial loss of the very high area of the dispersed platinum due to Ostwald ripening as a consequence of the lower solubility of Pt in the SPE;
- higher O_2 solubility and hence more effective transport of O_2 in the SPE;
- decreased adsorption of electrolyte components on the Pt catalyst, thus favoring O_2 adsorption.

The possibility exists that the electrochemical oxidation of the carbon substrate may be depressed with the SPE compared to the oxidation rate in concentrated H_3PO_4 without the SPE.

In place of solid ionomers such as Nafion, hydrogels can be used as the electrolyte within the active catalyst agglomerates. The authors have used quite successfully a hydrogel consisting of diallyl dimethyl ammonium polymer and Nafion, ion-paired through the tetra alkyl ammonium and sulfonate groups (22). The polymer gel can be formed within the already fabricated gas-fed porous electrode by infiltration with solutions of the polymer. The long term stability of the hydrogel, however, is open to question even in low temperature operation.

The long term chemical stability of ion exchange polymers with sulfonic acid groups also is uncertain at the operating temperatures of the phosphoric acid fuel cell ($\sim 200^\circ\text{C}$). To check on this question the infrared reflectance absorption spectra (IRRAS) of a 5 μm thick film of Dow 560 on Pt were examined in a modest vacuum ($\sim 10^{-4}$ Torr) at room temperature. The angle of incidence was 45° . The top spectrum in Fig. 17 was without heat treatment. The bottom spectrum was recorded after the sample had been held at 300°C for 7 h. The modes involving the sulfonic acid groups and water are greatly reduced in peak height while new modes involving ($\text{C}=\text{C}$) and ($=\text{C}-\text{F}$) appear. These measurements need to be carried out at temperatures of $\sim 200^\circ\text{C}$ at controlled potentials corresponding to the operating conditions of the O_2 cathode and also the H_2 anode. At 300°C , the stability of the polymer, particularly the sulfonic acid groups, would be a problem.

D. Structure of the Metal-Solid Polymer Electrolyte Interface

The structure of the Pt-SPE interface is uncertain. Attempts have been made to form polymer films on the surface of smooth Pt by applying a solution of the ionomer to the Pt surface and then evaporating out the solvent (usually an alcohol-water mixture). The films so prepared, however are not adherent. Adhesion can be greatly improved by heating the polymer film together with a small volume of dimethyl sulfoxide to $\sim 185^\circ\text{C}$, a procedure developed by Charles Martin and his students (23). Wilson and Gottesfeld (24) cast the film with the polymer in the Na form at 150 to 190°C in making the high area Pt catalyzed Nafion and this technique would probably lead to more stable films on smooth surfaces for fundamental studies of the film structure. The ionomer can then be converted to the acid form after fabrication is complete.

Chu (28) has found that the Nafion film is bonded better to the electrode if the film covers both the exposed disk surface and the flat plastic surface of the mounting.

The voltammograms for the Nafion films on smooth Pt and ordinary pyrolytic graphite (OPG) are very similar to those obtained without the polymer film in the same electrolytic solution. Furthermore the introduction of the $\text{Fe}^{2+}/\text{Fe}^{3+}$ couple into the bulk electrolyte results in the expected voltammetry behavior and rotating disk electrode results, taking into account the transport of the redox species through the Nafion film.

(30, 31). The voltammetry peak currents (without convection) are higher with the Nafion film due to the higher concentrations of Fe^{2+} and Fe^{3+} species in the film than in the corresponding bulk electrolyte solution (30). The mass transport corrected rotating disk polarization curves for O_2 reduction on smooth platinum are also almost the same with and without the Nafion layer on the platinum, although slightly improved with the polymer film (28).

On the Au electrode the thin Nafion film behaves quite differently. The dry film shows good adhesion without heat treatment in the acid form. In the voltammetry studies the formation of the anodic oxide film is delayed to more positive potentials (by, e.g., 0.3 V) and is much suppressed. The hydrogen overpotential is increased numerically. The double layer capacitance calculated from the non-Faradaic current and the sweep rate is reduced by a factor of 1/5. With bare Au, the $\text{Fe}^{2+}/\text{Fe}^{3+}$ couple shows relatively reversible behavior whereas with the Nafion film this couple is very irreversible. Only the reduction peak is evident with a peak shift in the cathodic direction of ~ -0.6 V at a sweep rate of 100mV/s.

The results for the Nafion film on Au are those expected with the hydrophobic fluorocarbon phase of the ionomer adjacent to the metal-polymer interface. On Pt and probably also OPG, the hydrophilic polar phase is predominant at the interface when the film is not thermally treated at temperatures of $\sim 180^\circ\text{C}$ or higher. Water transport through the hydrophilic phase appears to be very restricted.

Generally the kinetics of the O_2 reduction on Pt in acid electrolytes such as 0.7 M H_3PO_4 (23, 28) are faster with the duPont Nafion (117) or Dow ionomers covering the electrolyte surface. In contrast to the views of other workers, we do not believe that this difference is caused principally by the higher solubility of O_2 in the polymer layer but rather by the suppression of the concentration of H_2PO_4^- adjacent to the electrode in the polymer film and hence the suppression of the blocking of catalyst sites by this species. While the solubility of the O_2 in the hydrophobic phase is high, the solubility in the polar hydrophilic layer adjacent to the Pt surface is probably much lower and comparable to that in concentrated H_3PO_4 .

CONCLUSIONS

Only a few of the electrolyte factors listed in the Introduction have been discussed in detail in this paper. Some of these factors have a considerable effect on the kinetics of the O_2 reduction.

Some of the conclusions reached in this paper concerning the dependence of the kinetics on the electrolyte are as follows:

1. The role of protons in the O_2 reduction
 - Several types of evidence indicate that proton transfer is not involved in the rate determining step and is not an important factor in O_2 reduction kinetics in concentrated H_3PO_4 .
2. The competitive adsorption of O_2 vs. other components of the electrolytic solutions
 - This appears to be an important factor in explaining the difference between concentrated H_3PO_4 and the perfluoro sulfonic acids. The former contains phosphate species which strongly adsorb on Pt while the latter does not.
3. The effect of O_2 solubility in the electrolytic solution on O_2 reduction kinetics
 - Thermodynamics and absolute rate theory indicate that the O_2 solubility in the electrolytic solution should not have a direct effect on the rate of O_2 reduction at a fixed potential and a fixed O_2 partial pressure provided the O_2 reduction is not under mass transport control.
4. The effect of additives which form self assembled ordered films on Pt involving perfluorinated strong acids, such as the perfluoro sulfonimide and perfluoro carboxylic acids
 - The addition of even small amounts of these acids to concentrated H_3PO_4 lowers significantly the O_2 overpotential on both smooth and highly dispersed Pt. This decrease may be explained on the basis that the dielectric constant of the electrolyte side of the interfaces is decreased by the additive. This increases the adsorption of O_2 as a non-polar species and decreases the adsorption of polar species such as phosphate species and water itself.
5. The effects of a proton exchange ionomer layer on O_2 reduction kinetics on Pt
 - The O_2 reduction appears to be somewhat faster in acid electrolytes on Pt covered by a thin Nafion film layer. This effect may be explained on the basis that the film depresses the adsorption of the electrolyte components on the Pt catalyst. Only when mass transport of O_2 is at least partially controlling does O_2 solubility have a large effect on the O_2 reduction kinetics on Pt.
6. Structure of the metal-ionomer interface and its effects on the electrochemical properties of the interface
 - On Pt, the polymer phase adjacent to the electrode surface is predominantly the polar hydrophilic phase and the electrochemical behavior is essentially the same as with bare Pt in the same electrolyte solution with which the polymer was equilibrated. With gold the

hydrophobic phase is predominant and the electrochemical behavior is quite different from that of bare Au. The anodic film formation is depressed; the double layer capacity is decreased by $\sim 1/5$ and the $\text{Fe}^{2+}/\text{Fe}^{3+}$ couple becomes extremely irreversible. O_2 solubility is expected to be much lower in the polar regions than in the non-polar regions.

ACKNOWLEDGMENTS

The authors are pleased to acknowledge the contributions of their colleagues and graduate students to the research discussed in this paper, particularly Drs. D. Chu, S. Clouser, M. S. Hossain and E. O'Sullivan. Appreciation is expressed to the Gas Research Institute and the Office of Naval Research for the financial support of this research. The work benefitted from very helpful discussions with Dr. D. Scarpiello of the Gas Research Institute. The research on new acid electrolytes was made possible by the synthetic work of Prof. D. Des Marteau of Clemson University and Prof. D. Burton of Iowa University and their research groups.

LIST OF REFERENCES

- (1) S. Clouser, Ph.D. Thesis, Chemistry Department, Case Western Reserve University, Cleveland, Ohio, 1982.
- (2) J. C. Huang, R. K. Sen and E. Yeager, *J. Electrochem. Soc.*, **126**, 736 (1979).
- (3) J. P. Collman, P. Denisovich, Y. Konai, M. Marroco, C. Koval and F. Anson, *J. Am. Chem. Soc.*, **103**, 6027 (1980).
- (4) R. R. Durant, Jr., C. S. Bencosme, J. P. Collman and F. C. Anson, *J. Am. Chem. Soc.*, **105**, 2710 (1983).
- (5) M. Ghoneim, S. Clouser and E. Yeager, *J. Electrochem. Soc.*, **184** (1985) 1160.
- (6) D. Sepa, M. Voinovic and A. Damjanovic, *Electrochim. Acta*, **25**, 1491 (1980).
- (7) B. Conway in "Modern Aspects of Electrochemistry," **16**, 103 (1986).
- (8) B. R. Scharifker, P. Zelenay and J. O'M. Bockris, *J. Electrochem. Soc.*, **134**, 2713 (1987).
- (9) R. Kotz, S. Clouser, S. Sarangapani and E. Yeager, *J. Electrochem. Soc.*, **131**, 1097 (1984).
- (10) M. Enayetullah, E. O'Sullivan and E. Yeager, *J. Appl. Electrochem.*, **18** 763 (1988).
- (11) M. George and S. Januszkiewicz, Final Report, Energy Research Corp. Danbury, CT 06810; Report No. ERC-0123-F, June 1977.
- (12) M. Razaq, A. Razaq, E. Yeager, D. DesMarteau and S. Singh, *J. Applied Electrochem.*, **17**, 1057 (1987).
- (13) M. Razaq, A. Razaq, E. Yeager, D. DesMarteau and S. Singh, *J. Electrochem. Soc.*, **136**, 385 (1989).
- (14) C. P. Winlove, K. H. Parker and R.K.C. Oxenham, *J. Electroanal. Chem.* **170**, 293 (1984).

- (15) T.D. Gierke, "Ionic Clustering in Nafion Perfluorosulfonic Acid Membranes and Its Relationship to Hydroxyl Rejection and Chlor-Alkali Current Efficiency," Symposium on Perfluorocarbon Ion Exchange Membranes, National Meeting, The Electrochemical Society, Oct. 10-14, 1977, Atlanta, Proceedings, Published by Diamond Shamrock Corp., Cleveland and E. I. duPont Nemours & Co. (Inc.), Wilmington, Delaware.
- (16) M.W. Verbrugge and R.F. Hill, *J. Electrochem. Soc.*, **137**, 886 (1990).
- (17) M.W. Verbrugge and R.F. Hill, *J. Electrochem. Soc.*, **137**, 3770 (1990).
- (18) M.W. Verbrugge and R.F. Hill, *J. Electrochem. Soc.*, **137**, 1131 (1990).
- (19) R. Holze, A.T. Riga and E.B. Yeager, *J. Materials Science Letters*, **5**, 819 (1986).
- (20) J. Giner and C. Hunter, *J. Electrochem. Soc.*, **116**, 1124 (1969).
- (21) M. Watanabe, H. Sei and P. Stonehart, *J. Electroanal. Chem.*, **261**, 375 (1989).
- (22) A. Gordon, E. Yeager, D. Tryk and M.S. Hossain, Internat. Patent Publ. No. WO 88/06643, 7 Sept. 1988: Ionomer Membranes in Pressure Tolerant Gas Diffusion Electrodes; see also Internat. Patent Publ. No. WO 88/06645, 7 Sept. 1988: Hydrogel Loaded Active Layer in Pressure Tolerant Gas Diffusion Electrodes; Internat. Patent Publ. No. WO 88/06644, 7 Sept. 1988, Irradiated Ionomers on Pressure Tolerant Gas Diffusion Electrodes; Internat. Patent Publ. No. WO 88/06646, 7 Sept. 1988: Co-precipitated Hydrogels in Pressure Tolerant Gas Diffusion Electrodes.
- (23) M.S. Wilson and S. Gottesfeld, *J. Electrochem. Soc.*, **139**, 128 (1992).
- (24) R. Parsons, *J. Electroanal. Chem.*, **21**, 35 (1969).
- (25) D.R. Lawson, *J. Electrochem. Soc.*, **139**, 626 (1992).
- (26) S. Srinivasan, O.A. Velez, A. Parthasarathy, D. Manko and A. J. Appleby, *J. Power Sources*, **36**, 299 (1991).
- (27) D. Gervasio, M. Razaq, A. Razaq, K. Kanamura, R. Adzic and E. Yeager, "Electrochemical Characteristics of Acid Electrolytes for Fuel Cells," Final Report, Gas Research Institute, Contract 5084-260-1108, Case Western Reserve University, Cleveland, Ohio, Jan. 31, 1992.
- (28) D. Chu, Ph.D. Thesis, Chemistry Department, Case Western Reserve University, Cleveland, Ohio, 1989.
- (29) K.J. Laidler, "Chemical Kinetics," Chapters 3 and 5, McGraw Hill Book Co., New York, Second edition, 1965.
- (30) D. Chu, D. Tryk, D. Gervasio and E. Yeager, *J. Electroanal. Chem.*, **272**, 277 (1989).
- (31) D. Chu, D. Gervasio, M. Razaq, A. Razaq and E. Yeager, *J. Appl. Electrochem.*, **20**, 157 (1991).
- (32) E. Yeager, "Mechanisms of Electrochemical Reactions on Non-Metallic Surfaces" in National Bureau of Standards, Publ. 458, Electrocatalysis on Non-Metallic Surfaces, Washington, DC, 1976, pp. 203-219.

Table 1

Comparison of kinetic parameters for
O₂ reduction in CF₃SO₃H - H₃PO₄ - H₂O mixtures at 25°C (10)

Electrolyte H ₃ PO ₄ - CF ₃ SO ₃ H - H ₂ O (mol%)			i_d (mA/cm ²)	B (mA/cm ²)(rpm) ^{1/2}	$i \cdot i_d / (i_d - i)$ (mA/cm ²)	k_2/k_1 (at 0.80 V)
50	0	50	0.117	2.9×10^{-3}	5.3×10^{-2}	--
37.5	12.5	50	0.728	1.82×10^{-2}	5.38×10^{-2}	1.1
30.0	20.0	50	1.35	3.38×10^{-2}	15.1×10^{-2}	2.8
25.0	25.0	50	2.08	5.2×10^{-2}	31.4×10^{-2}	5.9

k_1 = rate constant for 50 mol% H₃PO₄ - 50 mol% H₂O (~86% H₃PO₄)

k_2 = rate constant for mixed acids

B = $0.62 n f D^{2/3} \nu^{-1/6} C_0$; obtained from Koutecky-Levich plots

i_d = diffusion limiting current density

Table 2

Oxygen Reduction at High Surface Area Electrodes
in Sulfonyl Acids and Bisphosphonic Acid Solutions

Electrolyte	Temperature [°C]	E - E 85% H ₃ PO ₄ [mV]		
		1	10	100 mA/cm ²
84% (FSO ₂) ₂ NH	70	-35	-105	-180
84% (CF ₃ SO ₂) ₂ NH	70	50	50	35
85% (PO(OH) ₂ CF ₂) ₂	100	100	70	50
85% H ₃ PO ₄ plus less than 0.1% (CF ₃ SO ₂ CH ₂ SO ₂ CF ₂ CF ₂) ₂	100	45	30	20
85% H ₃ PO ₄ plus 0.5% CF ₃ SO ₂ NHSO ₂ C ₄ F ₉	70	70	70	70

Table 3

The Solubility and Diffusivity of O₂ Determined using a
Pt Micro-Disk Electrode at 20°C in Various Electrolytes

Electrolytes	Solubility mol l ⁻¹	Diffusion coefficient cm ² s ⁻¹
85% H ₃ PO ₄	$3.3 \pm 0.4 \times 10^{-4}$	$1.27 \pm 0.5 \times 10^{-6}$
80% CF ₃ PO(OH) ₂	$3.7 \pm 0.2 \times 10^{-3}$	$1.44 \pm 0.2 \times 10^{-6}$
75% C ₂ F ₅ PO(OH) ₂	$6.0 \pm 0.3 \times 10^{-3}$	$1.6 \pm 0.3 \times 10^{-6}$
84% (CF ₃ SO ₂) ₂ NH	$3.8 \pm 0.2 \times 10^{-3}$	$6.53 \pm 0.3 \times 10^{-6}$
92% (C ₄ F ₉ SO ₂) ₂ NH	$1.6 \pm 0.1 \times 10^{-2}$	$4.40 \pm 0.1 \times 10^{-6}$
84% CF ₃ SO ₂ NHSO ₂ C ₄ F ₉	$4.7 \pm 0.2 \times 10^{-3}$	$5.97 \pm 0.2 \times 10^{-6}$
85% CF ₃ SO ₂ NHSO ₂ C ₆ F ₁₃	$5.4 \pm 0.2 \times 10^{-3}$	$6.87 \pm 0.1 \times 10^{-6}$
85% (CF ₂) ₃ (SO ₂) ₂ NH	$6.7 \pm 1 \times 10^{-3}$	$3.62 \pm 1 \times 10^{-6}$

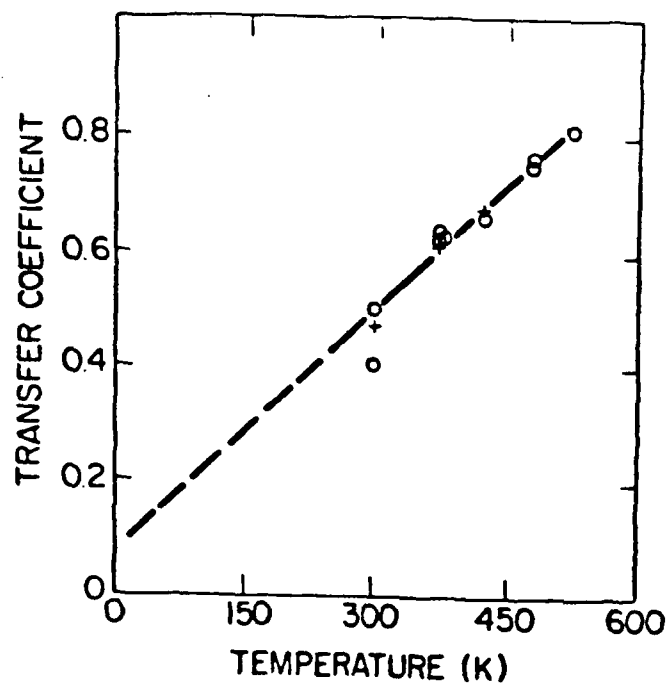


Fig. 1. Temperature dependence of apparent transfer coefficient α for O_2 reduction in concentrated H_3PO_4

O Clouser (1)
+ Huang et al. (2)

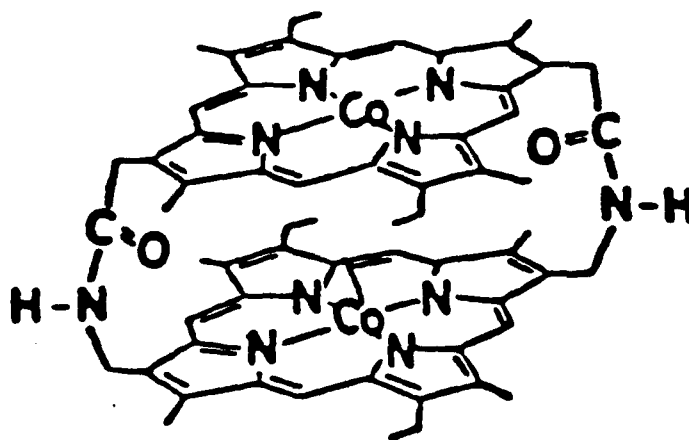


Fig. 2. Face-to-face Co-Co 4 porphyrin (3, 4)

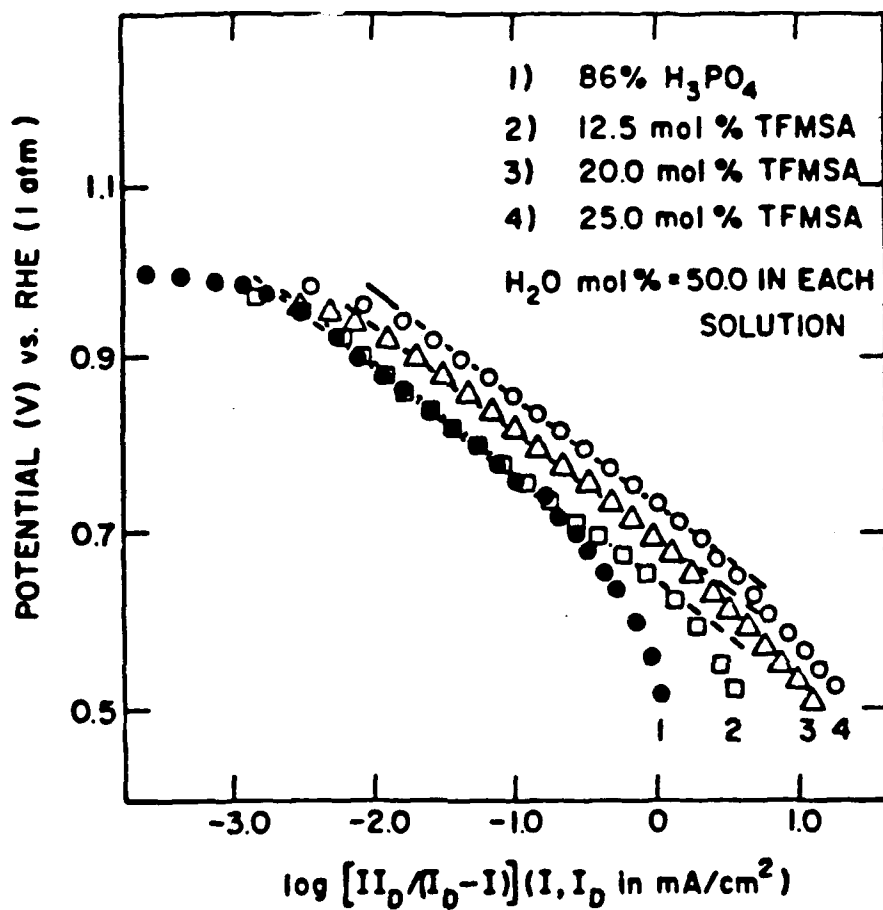


Fig. 3 Tafel plots for O_2 reduction in $\text{CF}_3\text{SO}_3\text{H}-\text{H}_3\text{PO}_4-\text{H}_2\text{O}$ mixtures and in 86% H_2PO_4 at 25°C . i_d values (mA cm^{-2}) are: (1) 0.116; (2) 0.728; (3) 1.35; (4) 2.08. Rotation rate = 1600 rpm (10).

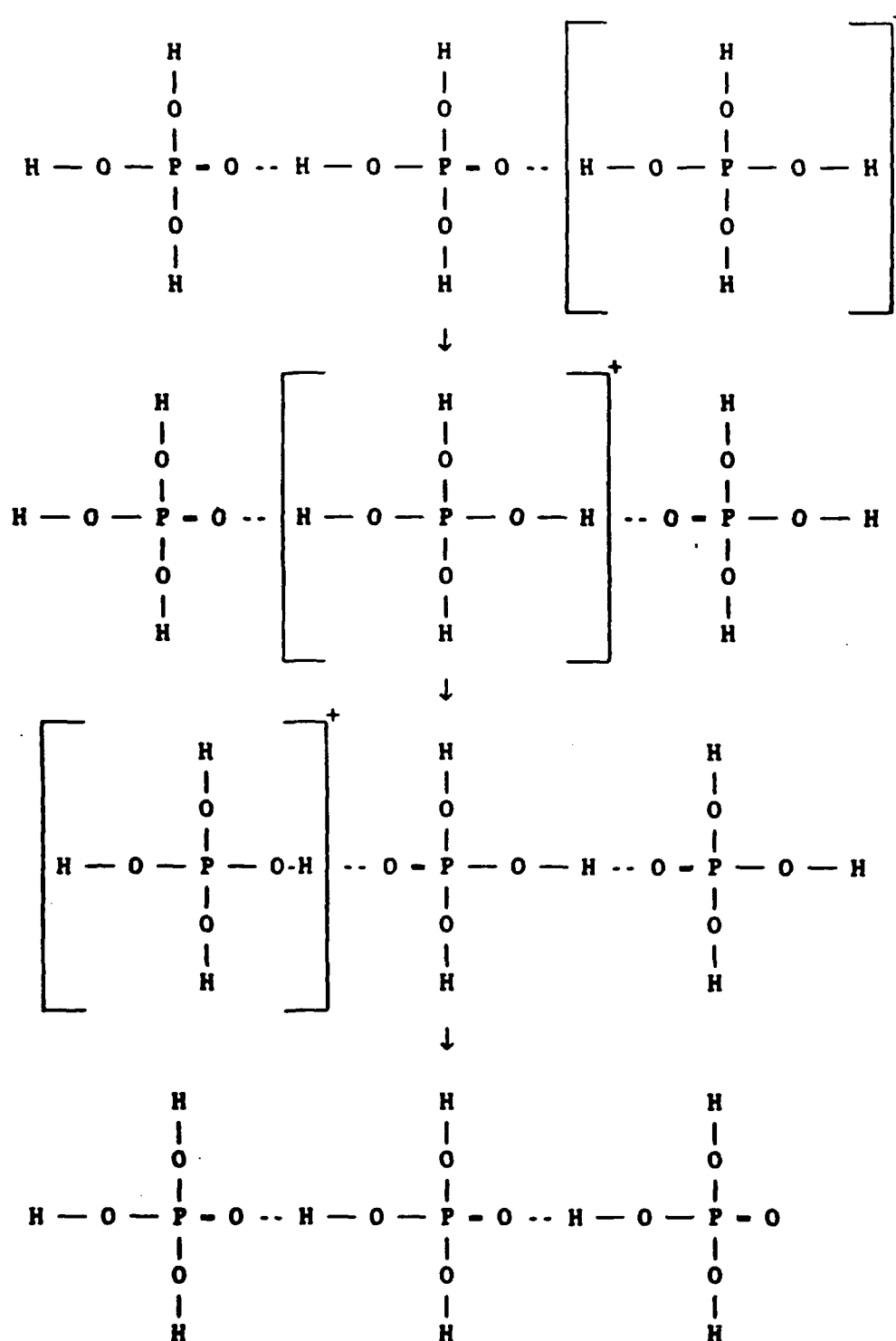


Fig. 4. Conduction mechanism in concentrated H_3PO_4 . The requirements for this Grotthius type conduction are hydrogen bonding network, (preferably three dimensional networks), partial ionization and short rotational diffusion relaxation time since diffusional rotation is required to re-arm the proton transfer system.

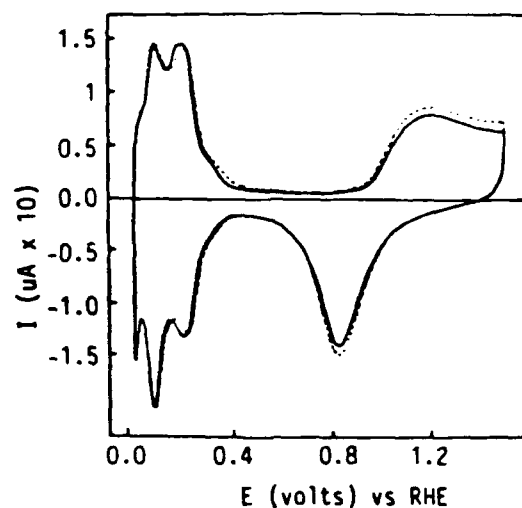


Fig. 5. Voltammograms of Pt in 85% H_3PO_4 (—) and 85% H_3PO_4 containing 4% PFSI (-----) solutions saturated with N_2 ; sweep rate = 100 mV s^{-1} ; electrode area = 0.126 cm^2 ; $T = 20^\circ\text{C}$.

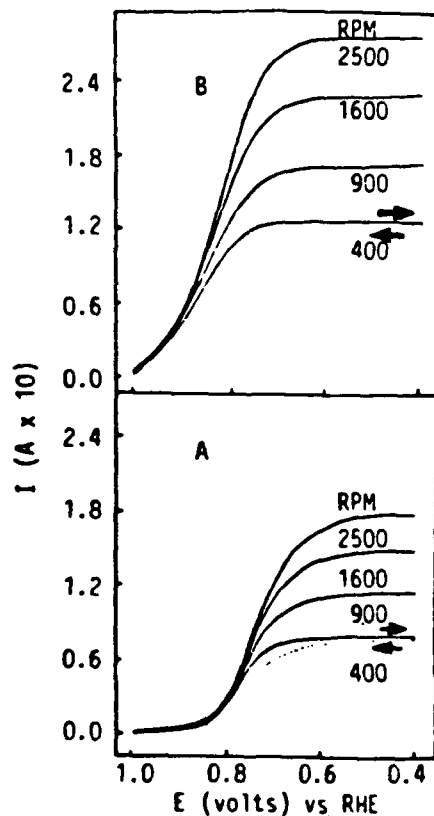


Fig. 6. (a) Polarization curves (12) for O_2 reduction on a Pt rotating disk electrode (area = 0.126 cm^2) in 85% H_3PO_4 ; solution saturated with O_2 at 1 atm; sweep rate = 10 mV s^{-1} ; $T = 20^\circ\text{C}$. (b) Solution 85% H_3PO_4 + 4% PFSI. Other conditions same as for Fig. 6a.

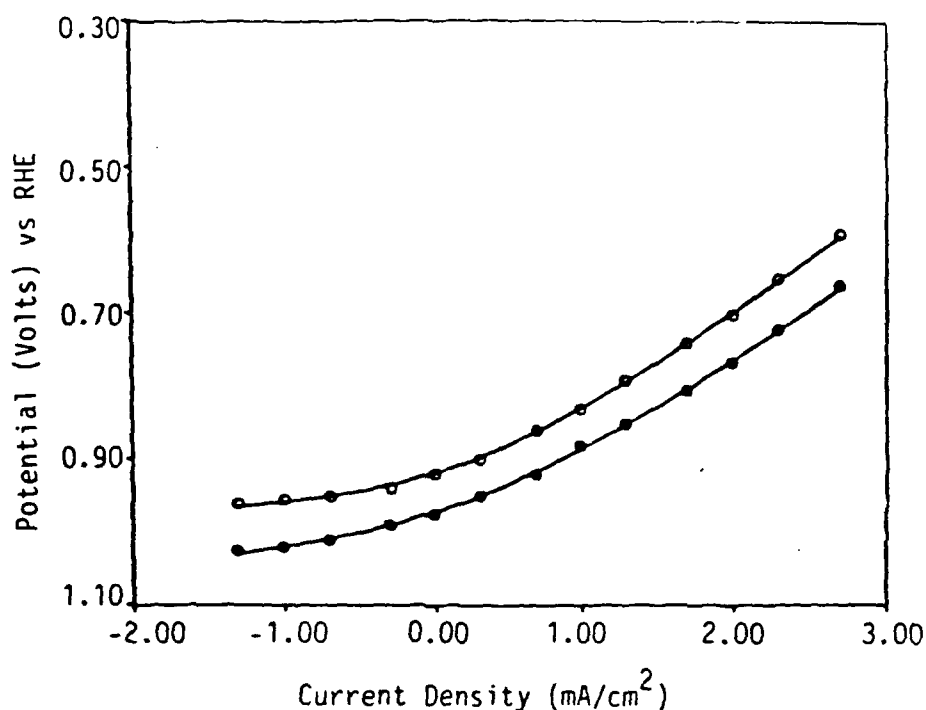


Fig. 7. Polarization curves for O₂ reduction on high-surface-area Prototech standard gas-fed electrode in 85% H₃PO₄ (O) and 85% H₃PO₄ containing 0.5% PFSI (●) at 70°C (13).

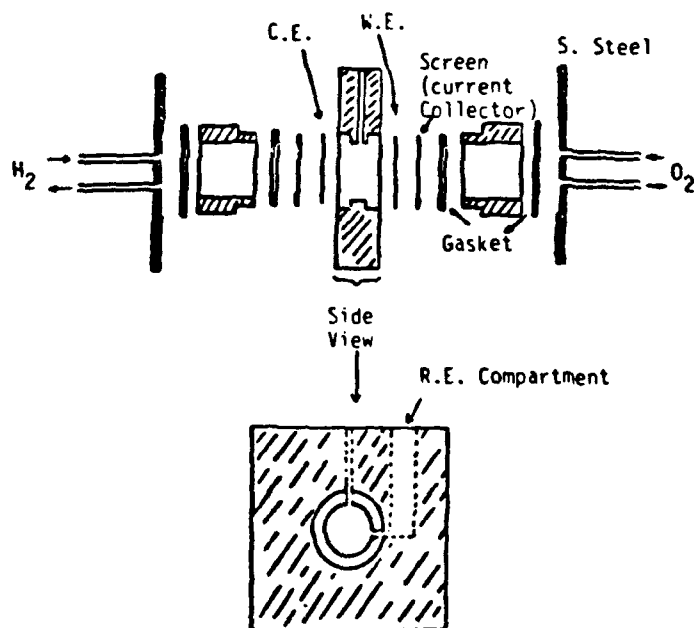


Fig. 8. Schematic representation of the micro-H₂ and O₂ fuel cell used to obtain polarization curves for gas-fed high area Pt cathodes.

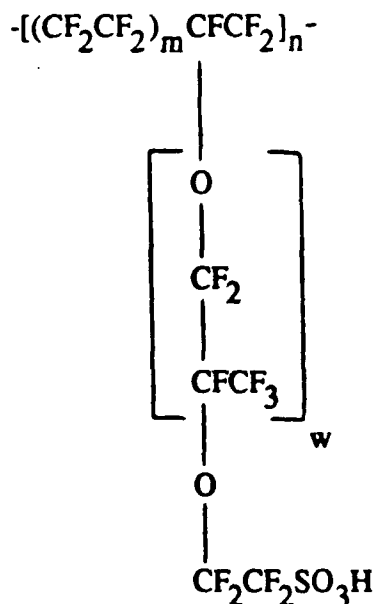


Fig. 9. Perfluorocarbon cation exchange polymers: duPont (Nafion) is available with various equivalent weights achieved by controlling the value of w . A typical value is 1100 (Nafion 117). Dow Chemical also has developed a similar sulfonic acid ionomer with an equivalent weight of 560 (Dow 560)

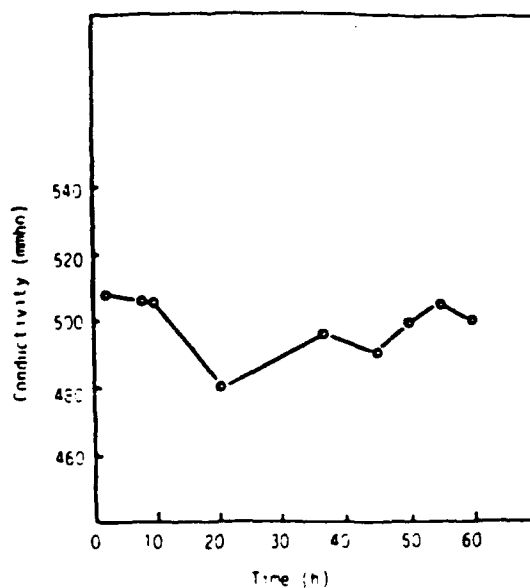


Fig. 10. Conductivity of duPont Nafion 117 membrane at 175°C as a function of time. The membrane was preequilibrated with H_3PO_4 by soaking it in 85% H_3PO_4 at 150°C for 12 h. The geometric area of the Prototech electrode in contact with the membrane was 2 cm².

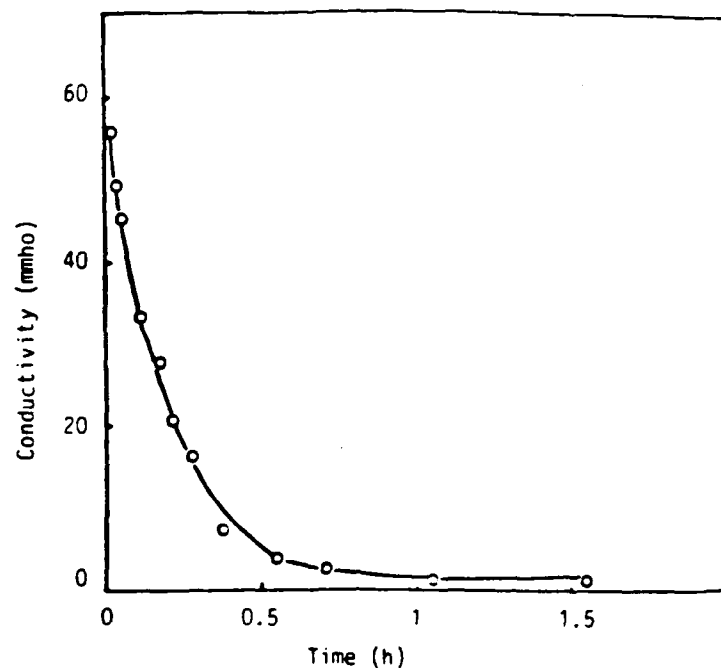


Fig. 11. Conductivity of Nafion 117 membrane at 100°C as a function of time. The membrane was preequilibrated with water by boiling the membrane in purified water. The electrode (Prototech gas-fed) had a geometric area in contact with the membrane of 2 cm².

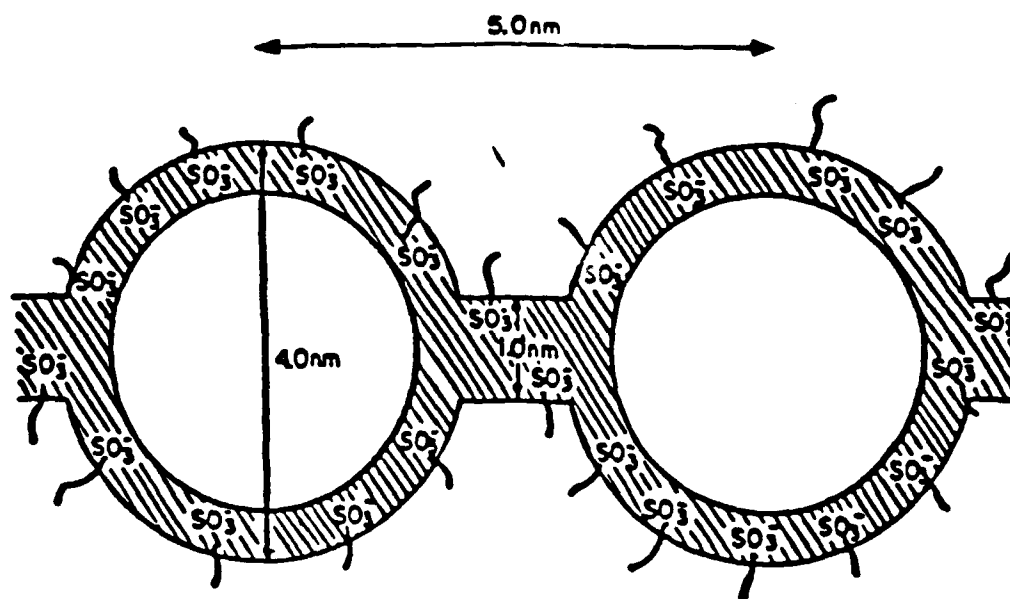


Fig. 12. Cluster-Network Model (15)

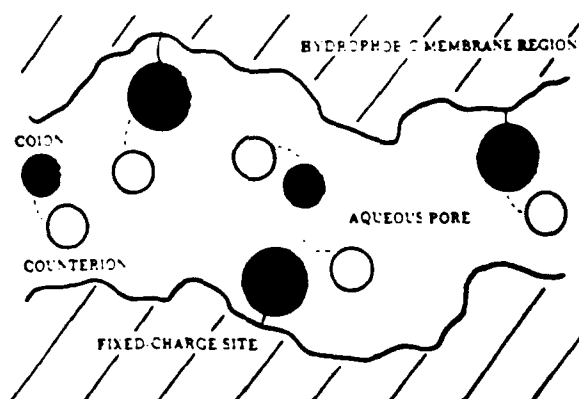


Fig. 13. Model of a channel with an ion-exchange membrane. O refers to the fixed charge sites (SO_3^-); o refers to the coions (HSO_4^-); and ● refers to the counterions (H^+). The fixed charge sites, coions, and counterions are hydrated species.

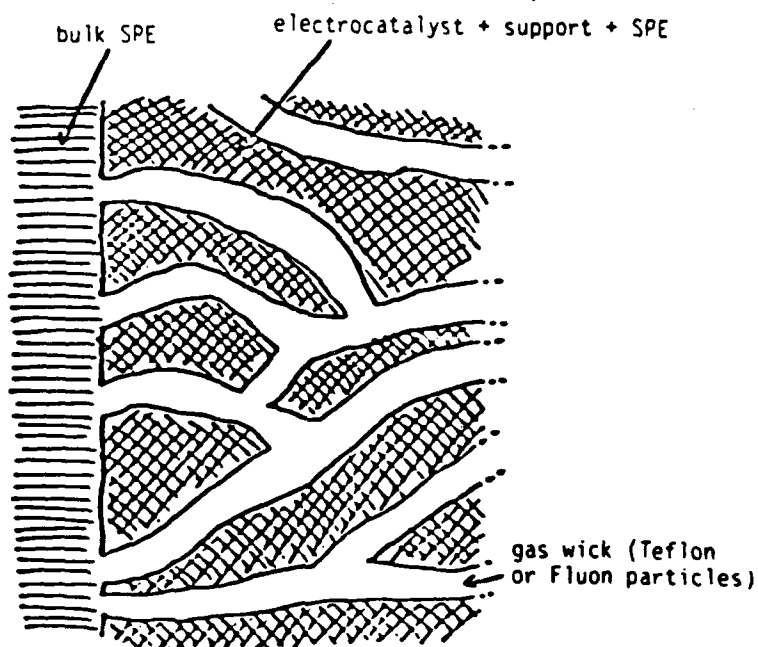


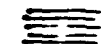


Fig. 14. Model of semi-hydrophobic gas-fed O_2 electrode using Nafion as the electrolyte.

-  Electrocatalyst-electronically conductive support-SPE agglomerates with a low concentration of PTFE particles to hold the phase together.
-  Teflon gas wicks
-  SPE alone

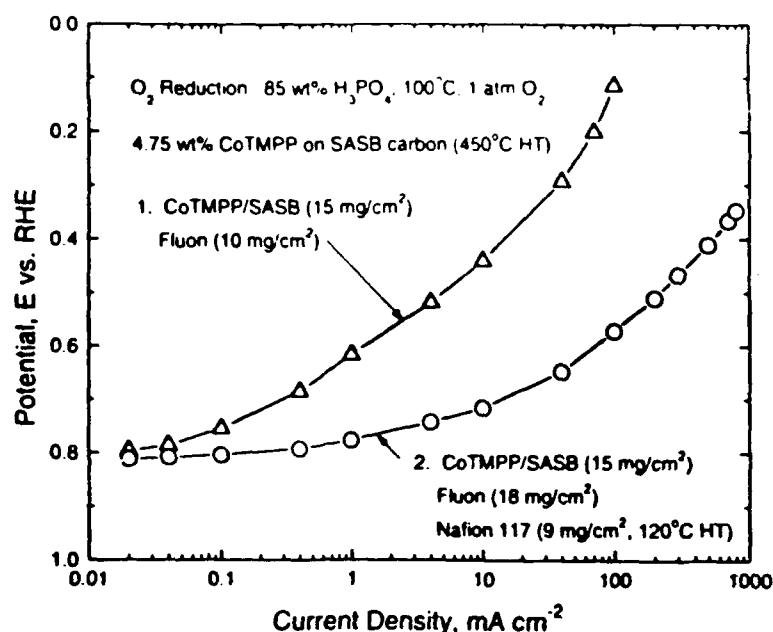


Fig. 15. Polarization curves for O_2 reduction in porous O_2 -fed (1 atm) electrodes in 85% H_3PO_4 at 100°C. Fluon (ICI) suspension with 0.24% perfluoro-octanoate stabilizer and 5% Nafion 117 (Aldrich) isopropanol suspension were used.

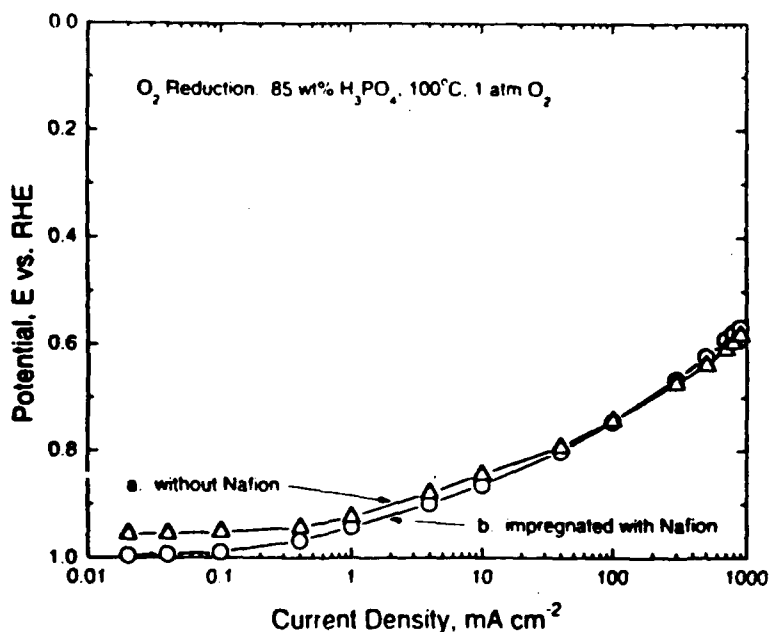


Fig. 16. Polarization curves for O_2 reduction at 100°C in 85% H_3PO_4 on a Prototech-fabricated Pt/C porous gas-diffusion active layer (Pt loading = 0.5 mg/cm²) with a carbon fiber-containing hydrophobic backing layer (Electromedia): a) without Nafion; b) impregnated with Nafion (Aldrich alcohol solution); Nafion loading = 10 mg/cm²; O_2 partial pressure = 1 atm.

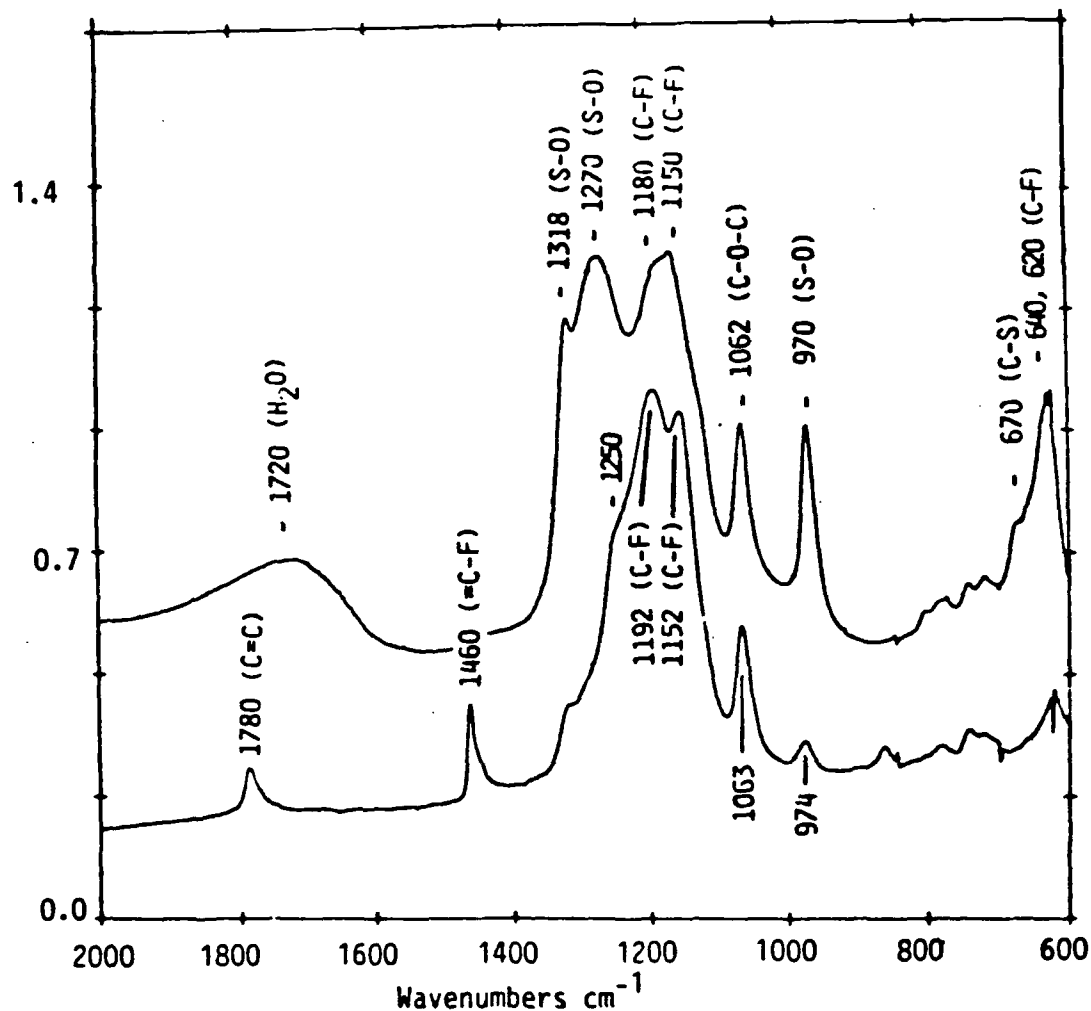


Fig. 17. Infrared reflection absorption spectra (IRRAS) of a 5 μm thick Dow 560 PFSI electrolyte film on Pt sampled in vacuum at room temperature. Angle of incidence of unpolarized radiation: 45° . Top spectrum: no heat treatment. Bottom spectrum: After heating the sample at 300°C for 7 hours in air.